Published in final edited form as:
Radiat Res. 2011 February ; 175(2): 172–184.

Identification of Radiation-Induced Expression Changes in Nonimmortalized Human T Cells

Era L. Pogosova-Agadjanyan[a], **Wenhong Fan**[b], **George E. Georges**[a,e], **Jeffrey L. Schwartz**[c], **Crystal M. Kepler**[a], **Hana Lee**[a], **Amanda L. Suchanek**[a], **Michelle R. Cronk**[a], **Ariel Brumbaugh**[a], **Julia H. Engel**[a], **Michi Yukawa**[d], **Lue P. Zhao**[b], **Shelly Heimfeld**[a], and **Derek L. Stirewalt**[a,e,1]

[a] Clinical Research Division, Fred Hutchinson Cancer Research Center, Seattle, Washington

[b] Program in Biostatistics and Biomathematics, Fred Hutchinson Cancer Research Center, Seattle, Washington

[c] Department of Radiation Oncology, University of Washington Medical Center, Seattle, Washington

[d] Department of Gerontology and Geriatric Medicine, University of Washington Medical Center, Seattle, Washington

[e] Division of Oncology, University of Washington Medical Center, Seattle, Washington

Abstract

In the event of a radiation accident or attack, it will be imperative to quickly assess the amount of radiation exposure to accurately triage victims for appropriate care. RNA-based radiation dosimetry assays offer the potential to rapidly screen thousands of individuals in an efficient and cost-effective manner. However, prior to the development of these assays, it will be critical to identify those genes that will be most useful to delineate different radiation doses. Using global expression profiling, we examined expression changes in nonimmortalized T cells across a wide range of doses (0.15–12 Gy). Because many radiation responses are highly dependent on time, expression changes were examined at three different times (3, 8, and 24 h). Analyses identified 61, 512 and 1310 genes with significant linear dose-dependent expression changes at 3, 8 and 24 h, respectively. Using a stepwise regression procedure, a model was developed to estimate *in vitro* radiation exposures using the expression of three genes (CDKN1A, PSRC1 and TNFSF4) and validated in an independent test set with 86% accuracy. These findings suggest that RNA-based expression assays for a small subset of genes can be employed to develop clinical biodosimetry assays to be used in assessments of radiation exposure and toxicity.

INTRODUCTION

In the event of a large-scale radiation accident or a terrorist attack, radiation dosimetry assays will be critical to the successful triage of patients for appropriate therapies. In addition, these assays and the knowledge gained from their development may lead to more precise methods of estimating toxicities to normal and diseased tissues. While the dicentric cytogenetic assays are the current gold standard for assessment of radiation dosimetry, these assays are labor-intensive, require mitotic cells, and may lack specificity at very low and

[1]Address for correspondence: Fred Hutchinson Cancer Research Center, Mailstop D5-112, P.O. Box 19024, 1100 Fairview Ave N, Seattle, WA 98109; dstirewa@fhcrc.org.

high doses (1,2). Thus there is a need to develop additional radiation dosimetry assays that are high-throughput, automated and cost-efficient (3).

Currently, there are numerous RNA-based clinical assays that risk-stratify patients with disease or assess the risk of disease development (4,5). These assays are quick, reliable and efficient. Furthermore, these assays can be readily automated using current robotic technology for high-throughput screening. RNA-based assays include global expression platforms, such as DNA microarrays, and more focused expression assessment via quantitative RT-PCR (qRT-PCR). Previous studies have found that DNA microarrays can be employed to identify and quantify thousands of radiation-induced expression changes within a single sample (6–17). Most microarray investigations have examined radiation-induced expression changes in malignant cell lines, immortalized human lymphoblastoid cells, and heterogeneous populations of primary cells, with the vast majority of these studies focusing on low and intermediate (≤4 Gy) doses (18–30), and in some cases, these expression signatures have been able to estimate radiation doses in unselected peripheral blood (31–36). Given the biological differences between immortalized and nonimmortalized cells, the limited range of radiation doses previously studied, and potential impact of cell heterogeneity on radiation-induced expression changes, there is a need to examine highly purified populations of nonimmortalized hematopoietic cells across an expansive range of radiation doses.

We examined the global expression profiles of homogeneous populations of nonimmortalized human T cells before and after exposure to a wide range of radiation doses (0–12 Gy). Due to the time-dependent nature of radiation responses, we studied the radiation-induced expression changes at multiple times (3, 8 and 24 h). The purpose of the study was to identify radiation-induced expression changes that are dose-dependent, and, more importantly, to build a model to estimate radiation exposure that can be used to estimate *in vivo* radiation exposures in a similar population of cells. In addition, the studies were designed to gain a better understanding of the expression changes associated with low and high doses of radiation, which may provide insight into the molecular biology of radiation responses and lead to the development of novel preventive approaches to blunt or reverse the unwanted effects of therapy-related radiation.

MATERIALS AND METHODS

Acquisition of Samples from Healthy Donors

Peripheral blood samples were collected from healthy volunteer donors at the Fred Hutchinson Cancer Research Center (FHCRC) or purchased from a commercial vendor (AllCells, Emeryville, CA). All samples were obtained under Institutional Review Board (IRB)-approved protocols, and consent was provided according to the Declaration of Helsinki. Donors were selected across a range of ages (23–61 years old), and there were roughly equivalent percentages of males (43%) and females (57%). Detailed donor information is provided in Supplementary Table 1.

Naive T-Cell Selection and Expansion

Mononuclear cells were separated from fresh peripheral blood using the Ficoll-Hypaque density gradient (37,38). Naïve T cells were purified on LS columns via dual negative selection using a CD4 selection kit II, followed by CD45RO immunomagnetic beads on a QuadroMax magnet according to manufacturer's specifications (Miltenyi Biotech, Auburn, CA) (37). The number of naïve T cells isolated from each sample is provided in Supplementary Table 1. The purity of naïve T cells ($CD4^+CD45RO^-$) was ≥90% by flow cytometry (37). To have adequate numbers of cells for the experiments, T cells were

expanded for 7 to 9 days with CD3/CD28 T-cell expander beads (Invitrogen, Carlsbad, CA) in X-vivo 15 medium without phenol red (Lonza, Walkersville, MD) supplemented with 5% FBS (HyClone, Logan, UT), 25 μg/ml gentamicin (Invitrogen) and 100 U/ml IL-2 (PeproTech, Rocky Hill, NJ) as described previously (37). After expansion, the T cells expressed a memory phenotype as a result of stimulation with CD3/CD28 beads and IL-2 (39–42).

In Vitro Irradiation of T-Cell Samples and RNA Extraction

Expanded T cells ($n = 8$) were exposed to ionizing radiation using a GammaCell 1000 Elite Irradiator (MDS Nordion, Kanata, Ontario, Canada) at an average rate of 7.6 Gy per minute at the following doses: 0 (sham), 0.15, 2, 4, 6, 9 and 12 Gy. After irradiation, the cells were cultured at 37°C in 95% air/5% CO_2 and harvested for RNA (TRIzol, Invitrogen, Carlsbad, CA) at 3, 8 and 24 h. Sham-irradiated samples (baseline controls) were collected at the time of exposure and 24 h after irradiation. RNA was extracted and assessed for quality as described previously (37,38,43).

In Vitro Irradiation of Whole Blood and Subsequent Cell Isolation

Whole blood samples from five donors were irradiated at 0 (sham), 2, 6 and 12 Gy as described above. After irradiation, the samples were kept at 37°C in 95% air/5% CO_2 and harvested 24 h later. White blood cells (granulocytes and mononuclear cells, WBCs) were separated using RBC lysis reagent (5-Prime/Fisher Scientific, Waltham, MA) and mononuclear cells (MNCs) were isolated using Histopaque-1077 (Sigma-Aldrich, St. Louis, MO) per the manufacturers' recommendations. A fraction of MNCs was positively selected for lymphocytes using magnetically labeled CD3 beads (Miltenyi) according to the manufacturer's recommendation. RNA was extracted from each of the three cell lysates using Trizol reagent (Invitrogen) per the manufacturer's recommendations (37,38).

DNA Microarrays and Statistical Analyses

Microarray processing—Five micrograms of total RNA was labeled using the Eukaryotic Target Labeling protocol, fragmented and hybridized (15 μg of biotin-labeled and fragmented antisense cRNA) onto HG-U133A arrays according to the Affymetrix protocol (Affymetrix, Santa Clara, CA) (37,38). DAT, CEL and CHP files were generated, and the results were screened for quality as described previously (37,38,44). Expression values for individual probe sets were generated using robust multi-array average (RMA), which generates background-adjusted, quantile-normalized log-transformed values (44,45). These $\log_2$-transformed expression values were imported into GenePlus™ software (Enodar Biologic, Seattle, WA) for downstream statistical analyses (37,38).

Baseline analysis—Expression profiles of sham-irradiated baseline control samples collected at 0 and 24 h postirradiation were evaluated to determine the independent effect of time on gene expression. Paired *t*-test analyses were performed for each available pair ($n = 7$ donors) and number of false discoveries (NFD) was used to select the significant probe sets (41–43). Expression changes were deemed to be statistically significant if the probe set displayed an NFD < 1.0 (46–48). Probe sets that displayed significant expression differences between the 0- and 24-h baseline samples were filtered out of the radiation-specific response analyses.

Dose-specific analyses—Dose-specific expression responses were identified by comparing the expression profiles of T cells exposed to low (0.15 Gy, E_{low}) or high (12 Gy, E_{high}) doses of radiation to sham-irradiated T cells (baseline control, C_B, 0 Gy). Due to the potential time-dependent nature of radiation-induced responses, analyses were performed

separately for each times. *T* tests were performed to generate the Z scores. The genes were further filtered for fold change, selecting genes with relative changes >1.2 or <0.83 (49). An *XY* plot displaying the Z scores from both analyses was generated for each time. The *XY* plot was then divided into nine quadrants using a Z score of ≥4.25 or ≤−4.25 as the cutoff for significance (46–48). Probe sets (i.e. genes) were deemed to be "low-dose specific" if they displayed both (1) a significant expression difference between E_{low} and C_B and (2) either no significant expression difference between E_{high} and C_B or a significant expression difference between E_{high} and C_B in the opposite direction. Probe sets were deemed to be "high-dose specific" if they displayed both (1) a significant expression difference between E_{high} and C_B and (2) either no significant expression difference between E_{low} and C_B or a significant expression difference in the opposite direction in this analysis.

Linear dose-dependent responses—Linear regression analyses were performed for 3, 8 and 24 h using radiation dose as a continuous independent variable (37). A multicovariate regression analysis was performed that incorporated gender, age (30–61), time (0, 3, 8 and 24 h after exposure), dose (0, 0.15, 2, 4, 6, 9 and 12 Gy) and dose*time interaction into the model (37). The results from the multicovariate regression analysis were used to confirm the linear regression results and to identify other covariates that may influence dose responses. NFD criteria were used to select the significant probe sets (41–43) such that probe sets displaying an NFD ≤ 1.0 were deemed to be statistically significant (46–48). If more than one probe set was deemed significant for a given gene, the probe set with the lowest NFD at 24 h was selected for future functional and canonical pathway analyses.

In silico comparison of low dose-dependent responses—Comparative analyses were performed examining reported genes with radiation-induced expression changes in *ex vivo* irradiated $CD4^+$ T cells (24). Mori *et al.* reported 48 genes with radiation-induced expression changes at 8 h after exposure in $CD4^+$T cells in response to 1 Gy. The expression of these 48 genes was assessed in our data using sham-irradiated controls and samples irradiated at 0.15 and 2 Gy. We limited the analyses to 8 h to parallel the experimental design of Mori *et al.* Expression changes were deemed to be statistically significant if the probe set displayed an NFD < 1.0 (46–48).

In silico comparison of linear dose-dependent responses—Linear regression analyses were performed using previously published microarray data (Gene Expression Omnibus, GSE701, HG-U95Av2) examining the radiation response of immortalized lymphoblastoid cells to 3 and 10 Gy at 24 h after exposure (22). CEL files were not available, so we used the author-supplied d-chip normalized data. The two array platforms were compared at the probe set level using the Affymetrix NetAffx Analysis Center to identify best-matched probe sets (www.affymetrix.com/analysis/index.affx). Since the d-chip normalized data included negative values, probe sets with at least one negative value were eliminated, leaving 5974 best-matched probe sets from four lymphoblastoid samples (two samples at 0 Gy, one each at 3 and 10 Gy). For these linear regression analyses, a Z score of 4.8 was considered significant.

Network Analyses

Affymetrix IDs and Z scores for the significant genes were loaded into the Ingenuity® Pathways Analysis (IPA) program (Ingenuity® Systems, www.ingenuity.com), and significant functional and canonical pathways were identified as described previously (37,38,50). All associations were supported by at least one literature reference and/or information from the Ingenuity Pathways Knowledge Base (51,52).

Validation of Microarray Studies by Quantitative RT-PCR

Quantitative RT-PCR (qRT-PCR) studies examined the expression of candidate genes in expanded T cells from an independent set of five donors using commercially available assays (Applied Biosystems, Foster City, CA) (37,38). For all expanded T-cell qRT-PCR studies, 500 ng of total RNA was reverse-transcribed with oligodT primer using AMV-RT according to the manufacturer's guidelines (Invitrogen). Fifty-nanogram cDNA equivalent was used for qRT-PCR assays, which were performed on StepOne Plus instrument (Applied Biosystems). For q-RT-PCR studies in nonexpanded cells, 100 ng of total RNA was reverse-transcribed as described above, and 10-ng cDNA equivalent per detector was assayed on ABI PRISM 7900 HT sequence detection system (Applied Biosystems). β-Glucoronidase (*GUSB*) was used as the endogenous control to correct for RNA integrity (53). The gene expression ratio was computed relative to the pool of RNA from the peripheral blood of seven healthy donors (the calibrator) using the $2^{-\Delta\Delta CT}$ method (53). Student's *t* test with one-tailed distribution and two-sample unequal variance was used to determine statistical significance. All assays were performed in triplicate with appropriate negative and positive controls.

Development and Validation of Radiations Dosimetry Model for T Cells

In vitro model development—For the development of the radiation dosimetry model, we examined the top six genes with radiation-induced expression changes using a stepwise regression procedure (SAS PROC REG). Radiation dose (0, 0.15, 2, 4, 6, 9 and 12 Gy) was set as the independent variable, and the dependent variable was the gene expression ratio. The significance cutoff for entry into the model was $P < 0.01$. The gene with the smallest *P* value entered the model first and then additional genes were added based upon their previous significance. Genes were removed from the model if they did not contribute significantly to dosimetry estimation (i.e., if their *P* value was >0.01). This model fitting procedure outputs a set of selected genes that are collectively the most robust for estimating radiation doses (54).

In vitro model testing—To determine the ability of the biodosimetry model to estimate *in vitro* radiation doses, we examined sensitivity and specificity of the model to estimate radiation doses in an independent set of samples at 24 h. For these studies, we examined *in vitro* radiation exposures across a similar range of doses (0, 0.15, 2, 4, 6, 9, 12 Gy). Gene expression ratios were obtained as described in the section on model development. Using these expression values, an estimated dose was calculated in a blinded manner for each sample. Then a 99.9% CI was calculated using the biodosimetry algorithm and compared to the actual radiation dose delivered. The accuracy was determined as the percentage of samples with the predicted dose calculated within the 99.9% CI of the actual dose relative to the total number of samples in the dose range.

RESULTS

Identification of Genes with Low- and High-Dose Radiation Responses

Radiation-induced expression changes were examined in a homogeneous population of nonimmortalized human T cells obtained from eight normal donors (age range 30–61, four males and four females). Supplementary Figs. 1 and 2A show cell viability across all doses at the 24 h and bioanalyzer electropherograms for all arrayed samples, respectively. The viability of the irradiated cells was directly proportional to the dose; however, the RNA from irradiated cells remained intact, with a degree of fluctuation in the ribosomal RNA ratio (55–57). The first set of studies examined differential expression between sham-irradiated samples collected at 0 and 24 h. The analyses identified 0.05% of probe sets (12 of 22,283) that displayed significant time-dependent expression changes without any exposure to

radiation (Supplementary Table 2, Supplementary Fig. 3). These probe sets were filtered out from the downstream radiation response analyses.

We then examined differences in radiation-induced expression changes between very low (0.15 Gy, E_{low}) and lethal (12 Gy, E_{high}) radiation doses. The expression profiles in T cells after E_{low} and E_{high} doses were directly compared to those for the sham-irradiated T cells (baseline control, C_B), and Z scores were plotted (Fig. 1A). Z scores provide both significance and directionality for expression changes (positive Z score indicates increased expression in the irradiated cells and vice versa). The low and high doses of radiation produced equivalent numbers of expression changes at the earlier time. The high dose produced more significant expression changes at 8 and 24 h, with an increasing number of significant genes over time (Fig. 1B–D). Summaries of the radiation-induced expression changes are provided in Table 1 and in Supplementary Tables 3A–3L. The detailed annotation of each array and CEL files are also available at the Gene Expression Omnibus (www.ncbi.nlm.nih.gov/geo).

We examined the functional pathways associated with radiation-induced expression changes using IPA software (37,38,50). At the transcriptional level, there was a considerable overlap between the functional pathways in the response to low- and high-dose exposures (Supplementary Table 4). Cell cycle regulation, cancer and cell death were the most significantly affected functions after both low- and high-dose exposures (all $P < 0.0001$). High-dose exposures tended to have a more dramatic impact on functional pathways than lower doses, which is consistent with the fact that high-dose exposures resulted in a greater number of significant radiation-induced expression changes than low-dose exposures (Fig. 1B and C). Specifically, high-dose exposures had a profound impact on DNA recombination/repair functions (Fig. 2A) and cell death (not shown). Some functional responses changed with time. In a few cases, the most pronounced effect was found early after exposure (e.g., cellular assembly/organization, Fig. 2B), while in most cases, the radiation-induced expression changes became more significant over time (e.g., cancer, Fig. 2C). These findings reiterate that many radiation-induced functional responses are quite dynamic and are dependent on time.

Similar analyses were performed to examine the time-dependent nature of canonical pathways. As with the functional analyses, there was considerable overlap in the significant canonical pathways after low- and high-dose exposures (Supplementary Table 5). For example, the PI3K/AKT, hypoxia, IL2 and T-cell receptor signaling pathways were affected to a similar degree after low- and high-dose exposures, particularly at 24 h (data not shown). However, just as with the functional analyses, more canonical pathways displayed significant radiation-induced expression changes after high doses than after low doses, and this dose effect was most pronounced at 24 h. The most dramatic example was the p53 signaling pathway. Low-dose exposures had only a marginal impact on the expression of genes in the p53 pathway at 3 h, while high-dose exposure resulted in more dramatic expression changes within this pathway that became more prominent with time (Fig. 2D). Not surprisingly, early after the high-dose exposure, there was an increase of transcriptional activity for genes involved in the G_1/S checkpoint pathway, which controls the entrance of cells into the DNA synthesis phase (Fig. 2E). A similar time-dependent effect was found for the glucocorticoid receptor signaling pathway (Fig. 2F). There were few if any canonical pathways with significant radiation-induced expression changes at the low dose that were not present at the high dose.

In Vitro Linear Dose-Dependent Radiation Responses

The low- and high-dose-specific results suggested a potential linear dose-dependent trend for many genes. Therefore, we performed univariate linear regression analyses for each time

for doses of 0, 0.15, 2, 4, 6, 9 and 12 Gy. The analyses identified 61, 512 and 1310 genes with significant linear dose-dependent expression changes at 3, 8 and 24 h, respectively (Fig. 3A). The lists of these significant genes are provided in Supplementary Tables 6G–H. Thirty-seven genes displayed similar dose-dependent changes in expression across all three times (Fig. 3B, top 10 genes—Table 2: all 37 genes—Supplementary Table 6A). As with the previous analyses, the number of genes with significant changes in expression increased with time. The radiation-induced expression changes for six of the most significant genes (CDKN1A, CDCA3, GADD45A, KIF20A, PSRC1 and TNFSF4; Supplementary Tables 6C–F) were confirmed by qRT-PCR in an independent donor population (five donors) at 24 h (Supplementary Table 6B, Supplementary Fig. 4).

These six top candidates were also evaluated in heterogeneous populations of WBCs (granulocytes + MNCs), MNCs and homogeneous population of positively selected nonexpanded lymphocytes (Table 3, Supplementary Fig. 2B). KIF20A did not show adequate amplification in any of the populations tested, suggesting that it is expressed at very low levels in nonexpanding cells. Three genes, CDCA3, GADD45A and TNFSF4, retained significant radiation-induced expression changes in all three populations studied. PSRC1 was of borderline significance in $CD3^+$ lymphocytes but showed no evidence of radiation-induced expression changes in WBCs or MNCs. TNFSF4 displayed the most robust linear dose-dependent change in expression ($R^2 = 0.67$, $P < 0.0001$) in the $CD3^+$ lymphocytes (Fig. 3C).

To examine the effect of other known variables on the dose-dependent responses, a multicovariate analysis was performed incorporating age, gender, time after exposure and dose. This analysis identified a total of 787 genes with linear dose-dependent responses (Supplementary Table 7B). Of the 787 genes, 11, 41 and 60 displayed significant associations with gender, age and time after exposure, respectively. Additional analyses identified 154 of the 787 genes that displayed a significant interaction between dose and time, indicating that the radiation-induced expression changes for these genes were highly dependent on the time after exposure (Fig. 3D). We then determined how many of the previously identified genes with significant linear dose-dependent responses also displayed significant radiation-induced expression changes in the multicovariate analyses, focusing on the 37 genes from the univariate analyses with radiation-induced expression changes conserved across all three times. All 37 genes (100%) were confirmed to have linear dose-dependent expression changes in the multicovariate regression model (Table 2, top 10 genes; Supplementary Table 7A contains all genes). However, several of these genes displayed changes in expression that were significantly associated with other variables. For example, *GADD45A*, *MDM2* and *PHLDA3* expression was associated with age of the donor ($NFD_{age} < 1$), and *GADD45A* and *MDM2* expression was also associated with gender ($NGD_{sex} < 1$). *TNFSF4* displayed a significant time and dose interaction ($NFD_{dose*time} < 1$), indicating that its expression was highly dependent upon the interval between exposure and testing.

To compare our results to other studies, we reviewed the literature to identify reports of radiation-induced expression changes in analogous populations of cells. Mori *et al.* identified 48 genes with radiation-induced expression changes between sham-irradiated control and 1 Gy-irradiated $CD4^+$ T cells (24). Of these, 44 genes were present on the HG-U133A array used in the present study. Seventy-seven percent of genes (34 of 44) displayed concordant expression changes and 23% (10 of 44) displayed discordant expression changes between the two data sets (Supplementary Tables 8A and B, respectively). Almost half of the genes with concordant radiation-induced expression changes (47%, 16 or 34) were statistically significant in our data, while less than a quarter of the genes with discordant radiation-induced expression changes were significant in our data set (20%, 2 of 10).

Another study by Jen *et al.* examined linear radiation-induced expression changes in lymphoblastoid cells (22). A total of 5974 genes displayed homology at the probe set level, allowing for direct comparison between the two platforms (Supplementary Fig. 5). Linear regression analyses found that 5% of the genes (306 of 5974) displayed significant concordant radiation-induced expression changes (i.e., significant increase or decrease in expression with radiation) in both data sets, while 1% of the genes (54 of 5974) displayed significant discordant changes (i.e., significant radiation-induced expression changes in both data sets, but in the opposite direction). Nine percent of the genes (519 of 5974) showed significant radiation-induced expression changes in the present study and not in the data set of Jen *et al.* and 28% of the genes (1663 of 5974) displayed significant radiation-induced expression changes in the study of Jen *et al.* but not in the present study. Information on these genes is provided in Supplementary Tables 9A–C.

Development and Validation of Radiation Dosimetry Model for T Cells

To investigate the potential use of radiation-induced expression changes in a T-cell biodosimetry assay, we developed a dose estimation model. The qRT-PCR expression ratios for the six most significant genes (CDCA3, CDKN1A, GADD45A, KIF20A, PSRC1 and TNFSF4) were analyzed using SAS PROC REG. These analyses focused on gene expression at 24 h after doses of 0, 0.15, 2, 4, 6, 9 and 12 Gy. CDKN1A, PSRC1 and TNFSF4 were found to be the most significant for estimating *in vitro* radiation doses in our T-cell training set (Fig. 4A). The regression dosimetry model was dose (Gy) = 2.637 + [1.047(CDKN1A) − 3.561(PSRC1) + 0.0586(TNFSF4)], where the gene symbol is the gene expression ratio.

We then tested the ability of the biodosimetry model to estimate the radiation dose under blinded conditions in an independent set of 21 samples from three donors across the same dose range. Overall, the regression biodosimetry model estimated doses ≤6 Gy extremely well (Fig. 4B), with 93% (14/15) of samples having an estimated dose within 2.2 Gy of the actual dose (99.9% CI). However, the dose estimation was less accurate for doses >6 Gy, with two of the six samples falling outside 2.2 Gy of the actual dose (Fig. 4C). Overall, the biodosimetry algorithm was 86% accurate in predicting the dose within 2.2 Gy of the actual dose.

DISCUSSION

We examined the radiation-induced expression changes across a wide range of doses in highly selected nonimmortalized human T cells and identified a large number of genes with radiation-induced expression changes. Overall, we found a dramatic increase in the number of radiation-induced expression changes at the higher doses. Likewise, there were more significant radiation-induced expression changes at 24 h than at 3 or 8 h. Given that radiation doses produce more severe damage per cell, it is logical that higher doses would cause more radiation-induced expression changes. However, it is unclear why radiation-induced expression changes increase in such a dramatic manner over time and at what time after irradiation radiation-induced expression changes will begin to dissipate and/or revert back to normal expression patterns. In addition, it is unknown whether the majority of the transcriptional changes are being translated into functional proteins, and if not, what the mechanism of this translational repression is. Given that we examined the responses only during the initial 24 h after exposure, additional studies will be required to answer some of these questions. It is intriguing that the RNA findings are in sharp contrast to the immediate protein phosphorylation responses, which may dissipate within 4–8 h after exposure (58,59). Overall, the data suggest that RNA-based assays may provide an excellent method to estimate radiation doses within the first 24 h after exposure.

There were a number of genes that displayed similar expression changes after both low- and high-dose exposures. In particular, low- and high-dose exposures caused radiation-induced expression changes in genes associated with cell cycle regulation, cancer and cell death, all of which have been implicated previously in radiation responses (60–63). However, we also found many genes with significant expression differences between the low (0.15 Gy) and high (12 Gy) doses. Informatic analyses revealed that these "dose-specific" radiation-induced expression changes were often associated with specific functional and canonical pathways (Figs. 1 and 2). Many of these dose-specific radiation-induced expression changes were also highly dependent on time. Overall, a more robust effect at the RNA level on most functional and canonical pathways was observed at higher doses, especially DNA recombination/repair, G_1/S checkpoint regulation, and p53 signaling, and these effects generally were greatest at 24 h (Fig. 2). However, one must be cautious of any biological or functional pathway analyses based on RNA expression, since most of the functional attributes are driven by the proteome. Additional studies examining radiation-induced proteomic changes are warranted and may expand our knowledge of the biology of radiation response.

We identified a large number of genes with linear radiation-induced expression changes, 37 of which expressed similar robust dose-dependent changes at 3, 8 and 24 h. The six genes with the most significant radiation-induced expression changes were CDKN1A, GADD45A, TNFSF4, KIF20A, PSRC1 and CDCA3. These linear dose-dependent expression changes were validated by qRT-PCR in an independent population of homogeneous T cells. Expression of CDKN1A, GADD45A and TNFSF4 was induced in a dose-dependent manner, as has been reported previously in different types of cells, tissues and organisms (6,22,24,31,64–69). The three repressed genes (KIF20A, PSRC1 and CDCA3) have not previously been shown to be responsive to radiation damage. KIF20A is a kinesin involved in chromosome segregation and mitosis (70,71). CDCA3 is a trigger of mitotic entry (72–75). PSRC1 is a p53 target that controls spindle dynamics and mitotic chromosome movement (76–79). Given the direct involvement of these repressed genes in mitosis, their diminished transcription may be expected to be a logical outcome after DNA-damaging effects of radiation (62,68,80–82).

To investigate the similarities and differences between our results and those of others, we examined the transcriptional responses in our study and that of Mori *et al.* (24). Overall, there was a significant amount of overlap between the two data sets, with the majority of the genes (77%) displaying concordant radiation-induced expression changes. This high concordance is quite striking given the differences in the array platforms (oligonucleotide vs. spotted arrays), radiation doses used (0.15 and 2 Gy vs. 1 Gy), and manipulations of T cells (naive, $CD4^+CD45RO^-$, expanded T cells vs. $CD4^+$ cells) between our and data sets and those of Mori *et al*.

We further explored similarities and differences in linear radiation-induced expression changes between nonimmortalized T cells and lymphoblastoid cells (22) and found a relatively modest level of significant concordant radiation-induced expression changes (5%) between the two populations, with very few (1%) significant discordant changes. The vast majority of the genes that were significant in one population were not significant in the other. There are many possible reasons for the limited amount of overlap between the two data sets. The two studies used different platforms and normalization parameters. There may also be significant biological differences between nonimmortalized T cells and lymphoblastoid cells. However, further analyses suggest that many of these genes displayed modest concordant radiation-induced expression changes that did not reach statistical significance. For example, 71% (367/520) of the genes with significant radiation-induced

expression changes in nonimmortalized T cells also displayed similar transcriptional responses in the lymphoblastoid cells.

The optimal cell population for examining radiation-induced expression changes remains uncertain. In this study we examined a homogeneous population of cells that may not be easily accessible for high-throughput evaluation of radiation response. A less homogeneous population, such as peripheral blood leukocytes, might have similar or more robust radiation-induced expression changes. To investigate this possibility and the generalizability of our findings, we examined the expression of selected genes in WBCs, MNCs and $CD3^+$ cells, none of which underwent expansion. We found that some of the genes displayed more pronounced and robust radiation-induced expression changes in the lymphocyte population (e.g. TNFSF4), while others (e.g. GADD45A) displayed similar if not more pronounced radiation-induced expression changes in the heterogeneous population of cells. These data suggest that some radiation-induced expression changes will be more cell type-specific than others.

Due to the ever increasing threat of unintended and intended radiation exposure, there is a need to develop high-throughput radiation dosimetry assays. Prior to the development of such assays, one must first identify potential candidate genes that can accurately discriminate between different doses of radiation. We hypothesized that genes with linear dose-dependent expression changes expression will be useful in the development of biodosimetry models to estimate radiation dose. Using the expression of CDKN1A, PSRC1 and TNFSF4, we developed a biodosimetry model that was 86% accurate in estimating previous *in vitro* exposures within 2.2 Gy (99.9% CI). Two of the three blinded samples that were wrongly classified received higher radiation doses (>6 Gy). Paul *et al.* also noted decreased accuracy in the ability to estimate higher doses of radiation using RNA-based approaches (31). These investigators used a 74-gene panel to estimate radiation dose in a heterogeneous population of peripheral blood cells, obtaining 78% accuracy to correctly classify previous exposures. Similar to our study, they found that the majority of incorrectly classified samples were in the higher-dose range (>5 Gy). While our biodosimetry model estimates lower doses fairly well, this assay may have less discriminatory power to estimate high-dose exposure. In the case of high-dose exposures, multiple genes, other biomarkers and/or clinical findings may need to be combined with RNA-based assays to risk-stratify victims accurately.

Ideally, genes selected for biodosimetry models will exhibit dose-dependent changes that are independent of age, gender, time, cell type and/or other potential interindividual confounders. Dosimetry assays using such targets could be widely implemented and interpreted across various human populations and under potentially infinite exposure scenarios. Our multicovariate analyses found that expression of many genes with radiation dose-dependent responses was associated with other variables such as age, time and/or gender. For example, the expressions of PHLDA3 and GADD45A, two genes with robust radiation-induced expression changes in our analyses, were also significantly associated with age. Similarly, many if not most genes with radiation-induced expression changes displayed expression changes that were highly dependent upon the time after exposure, even if this association was modest (Fig. 3C).

Our findings provide insight into the heterogeneity of radiation responses due to interindividual biological variations, but the results highlight yet another level of complexity to be considered when developing radiation dosimetry assays. Future dosimetry studies will have to account for interindividual differences (e.g., age, gender, etc.), environmental circumstances (e.g., partial exposures), cell type and mode and rate of delivery of radiation (e.g., source, dose rate, etc.). To evaluate and correct for all these variables, further studies

are necessary. These additional studies will likely examine larger populations of subjects in *ex vivo* and *in vivo* models. Such studies are planned by our and other groups.

In summary, we have identified a large number of genes with radiation-induced expression changes in a nonimmortalized, homogeneous population of T cells. Furthermore, we were able to develop a radiation dosimetry model using the expression of three genes that estimated the *in vitro* dose with 86% accuracy. This algorithm was most informative at low to moderate radiation doses. Although these results are promising, there are limitations to these studies. To obtain sufficient cell numbers, the naiïve T cells were expanded and were actively dividing in a culture system at the time of irradiation. The expression signature after irradiation may differ between activated cells and homeostatic cells in the peripheral blood. Also, our studies were performed using an *in vitro* model, which cannot approximate the complex microenvironment and macro-environment of the human hematopoietic system. Last, the radiation-induced expression changes were examined across eight individual donors, limiting our capacity to control and correct for interindividual confounders. These limitations reiterate the need to examine gene expression signatures in a larger cohort of donors, addressing interindividual and environmental contributions to dose-dependent expression changes and selecting the targets that are least affected by these variables. Also, it will be important to determine how these radiation-induced expression changes, which were identified in a highly homogeneous population of non-immortalized T-cells, may be generalizable to other populations of hematopoietic cells and whole blood.

Supplementary Material

Refer to Web version on PubMed Central for supplementary material.

Acknowledgments

This work was supported by NIH/NIAID grant number U19 AI067770.

References

1. Amundson SA, Bittner M, Meltzer P, Trent J, Fornace AJ Jr. Biological indicators for the identification of ionizing radiation exposure in humans. Expert Rev Mol Diagn. 2001; 1:211–219. [PubMed: 11901816]
2. Blakely WF, Salter CA, Prasanna PG. Early-response biological dosimetry—recommended countermeasure enhancements for mass-casualty radiological incidents and terrorism. Health Phys. 2005; 89:494–504. [PubMed: 16217193]
3. Pellmar TC, Rockwell S. Priority list of research areas for radiological nuclear threat countermeasures. Radiat Res. 2005; 163:115–123. [PubMed: 15606315]
4. Keilholz U, Letsch A, Busse A, Asemissen AM, Bauer S, Blau IW, Hofmann WK, Uharek L, Thiel E, Scheibenbogen C. A clinical and immunological phase II trial of Wilms tumor gene product 1 (WT1) peptide vaccination in patients with AML and MDS. Blood. 2009; 113:6541–6548. [PubMed: 19389880]
5. Druker BJ, Guilhot F, O'Brien SG, Gathmann I, Kantarjian H, Gattermann N, Deininger MW, Silver RT, Goldman JM, Larson RA. Five-year follow-up of patients receiving imatinib for chronic myeloid leukemia. N Engl J Med. 2006; 355:2408–2417. [PubMed: 17151364]
6. Amundson SA, Lee RA, Koch-Paiz CA, Bittner ML, Meltzer P, Trent JM, Fornace AJ Jr. Differential responses of stress genes to low dose-rate gamma irradiation. Mol Cancer Res. 2003; 1:445–452. [PubMed: 12692264]
7. Vilenchik MM, Knudson AG Jr. Inverse radiation dose-rate effects on somatic and germ-line mutations and DNA damage rates. Proc Natl Acad Sci USA. 2000; 97:5381–5386. [PubMed: 10792040]

8. Kumar PR, Mohankumar MN, Hamza VZ, Jeevanram RK. Dose-rate effect on the induction of HPRT mutants in human G_0 lymphocytes exposed in vitro to gamma radiation. Radiat Res. 2006; 165:43–50. [PubMed: 16392961]
9. Vilenchik MM, Knudson AG. Radiation dose-rate effects, endogenous DNA damage, and signaling resonance. Proc Natl Acad Sci USA. 2006; 103:17874–17879. [PubMed: 17093045]
10. Amundson SA, Chen DJ. Inverse dose-rate effect for mutation induction by gamma-rays in human lymphoblasts. Int J Radiat Biol. 1996; 69:555–563. [PubMed: 8648243]
11. Mothersill C, Kadhim MA, O'Reilly S, Papworth D, Marsden SJ, Seymour CB, Wright EG. Dose– and time–response relationships for lethal mutations and chromosomal instability induced by ionizing radiation in an immortalized human keratinocyte cell line. Int J Radiat Biol. 2000; 76:799–806. [PubMed: 10902734]
12. Fournier C, Taucher-Scholz G. Radiation induced cell cycle arrest: an overview of specific effects following high-LET exposure. Radiother Oncol. 2004; 73(Suppl. 2):S119–S122. [PubMed: 15971325]
13. Ross HJ, Canada AL, Antoniono RJ, Redpath JL. High and low dose rate irradiation have opposing effects on cytokine gene expression in human glioblastoma cell lines. Eur J Cancer. 1997; 33:144–152. [PubMed: 9071914]
14. Wu L, Levine AJ. Differential regulation of the p21/WAF-1 and mdm2 genes after high-dose UV irradiation: p53-dependent and p53-independent regulation of the mdm2 gene. Mol Med. 1997; 3:441–451. [PubMed: 9260156]
15. Li G, Ho VC. p53-dependent DNA repair and apoptosis respond differently to high- and low-dose ultraviolet radiation. Br J Dermatol. 1998; 139:3–10. [PubMed: 9764141]
16. Lind BK, Persson LM, Edgren MR, Hedlof I, Brahme A. Repairable-conditionally repairable damage model based on dual Poisson processes. Radiat Res. 2003; 160:366–375. [PubMed: 12926995]
17. Rothkamm K, Lobrich M. Evidence for a lack of DNA double-strand break repair in human cells exposed to very low x-ray doses. Proc Natl Acad Sci USA. 2003; 100:5057–5062. [PubMed: 12679524]
18. Amundson SA, Bittner M, Chen Y, Trent J, Meltzer P, Fornace AJ Jr. Fluorescent cDNA microarray hybridization reveals complexity and heterogeneity of cellular genotoxic stress responses. Oncogene. 1999; 18:3666–3672. [PubMed: 10380890]
19. Amundson SA, Do KT, Fornace AJ Jr. Induction of stress genes by low doses of gamma rays. Radiat Res. 1999; 152:225–231. [PubMed: 10453082]
20. Jaworska A, Szumiel I, De Angelis P, Olsen G, Reitan J. Evaluation of ionizing radiation sensitivity markers in a panel of lymphoid cell lines. Int J Radiat Biol. 2001; 77:269–280. [PubMed: 11258841]
21. Guo WF, Lin RX, Huang J, Zhou Z, Yang J, Guo GZ, Wang SQ. Identification of differentially expressed genes contributing to radioresistance in lung cancer cells using microarray analysis. Radiat Res. 2005; 164:27–35. [PubMed: 15966762]
22. Jen KY, Cheung VG. Transcriptional response of lymphoblastoid cells to ionizing radiation. Genome Res. 2003; 13:2092–2100. [PubMed: 12915489]
23. Akerman GS, Rosenzweig BA, Domon OE, Tsai CA, Bishop ME, McGarrity LJ, Macgregor JT, Sistare FD, Chen JJ, Morris SM. Alterations in gene expression profiles and the DNA-damage response in ionizing radiation-exposed TK6 cells. Environ Mol Mutagen. 2005; 45:188–205. [PubMed: 15657912]
24. Mori M, Benotmane MA, Vanhove D, van Hummelen P, Hooghe-Peters EL, Desaintes C. Effect of ionizing radiation on gene expression in $CD4^+$ T lymphocytes and in Jurkat cells: unraveling novel pathways in radiation response. Cell Mol Life Sci. 2004; 61:1955–1964. [PubMed: 15341025]
25. Long XH, Zhao ZQ, He XP, Wang HP, Xu QZ, An J, Bai B, Sui JL, Zhou PK. Dose-dependent expression changes of early response genes to ionizing radiation in human lymphoblastoid cells. Int J Mol Med. 2007; 19:607–615. [PubMed: 17334636]
26. Short SC, Buffa FM, Bourne S, Koritzinsky M, Wouters BG, Bentzen SM. Dose- and time-dependent changes in gene expression in human glioma cells after low radiation doses. Radiat Res. 2007; 168:199–208. [PubMed: 17638411]

27. Lin R, Sun Y, Li C, Xie C, Wang S. Identification of differentially expressed genes in human lymphoblastoid cells exposed to irradiation and suppression of radiation-induced apoptosis with antisense oligonucleotides against caspase-4. Oligonucleotides. 2007; 17:314–326. [PubMed: 17854271]
28. Tsai MH, Cook JA, Chandramouli GV, DeGraff W, Yan H, Zhao S, Coleman CN, Mitchell JB, Chuang EY. Gene expression profiling of breast, prostate, and glioma cells following single versus fractionated doses of radiation. Cancer Res. 2007; 67:3845–3852. [PubMed: 17440099]
29. Amundson SA, Do KT, Vinikoor LC, Lee RA, Koch-Paiz CA, Ahn J, Reimers M, Chen Y, Scudiero DA, Fornace AJ Jr. Integrating global gene expression and radiation survival parameters across the 60 cell lines of the National Cancer Institute Anticancer Drug Screen. Cancer Res. 2008; 68:415–424. [PubMed: 18199535]
30. Mahmoud-Ahmed AS, Atkinson S, Wong CS. Early gene expression profile in mouse brain after exposure to ionizing radiation. Radiat Res. 2006; 165:142–154. [PubMed: 16435913]
31. Paul S, Amundson SA. Development of gene expression signatures for practical radiation biodosimetry. Int J Radiat Oncol Biol Phys. 2008; 71:1236–1244. [PubMed: 18572087]
32. Kang CM, Park KP, Song JE, Jeoung DI, Cho CK, Kim TH, Bae S, Lee SJ, Lee YS. Possible biomarkers for ionizing radiation exposure in human peripheral blood lymphocytes. Radiat Res. 2003; 159:312–319. [PubMed: 12600233]
33. Svensson JP, Stalpers LJ, Esveldt-van Lange RE, Franken NA, Haveman J, Klein B, Turesson I, Vrieling H, Giphart-Gassler M. Analysis of gene expression using gene sets discriminates cancer patients with and without late radiation toxicity. PLoS Med. 2006; 3:e422. [PubMed: 17076557]
34. Meadows SK, Dressman HK, Muramoto GG, Himburg H, Salter A, Wei Z, Ginsburg GS, Chao NJ, Nevins JR, Chute JP. Gene expression signatures of radiation response are specific, durable and accurate in mice and humans. PLoS One. 2008; 3:e1912. [PubMed: 18382685]
35. Dressman HK, Muramoto GG, Chao NJ, Meadows S, Marshall D, Ginsburg GS, Nevins JR, Chute JP. Gene expression signatures that predict radiation exposure in mice and humans. PLoS Med. 2007; 4:e106. [PubMed: 17407386]
36. Rieger KE, Chu G. Portrait of transcriptional responses to ultraviolet and ionizing radiation in human cells. Nucleic Acids Res. 2004; 32:4786–4803. [PubMed: 15356296]
37. Stirewalt DL, Choi YE, Sharpless NE, Pogosova-Agadjanyan EL, Cronk MR, Yukawa M, Larson EB, Wood BL, Appelbaum FR, Heimfeld S. Decreased IRF8 expression found in aging hematopoietic progenitor/stem cells. Leukemia. 2008; 23:391–393. [PubMed: 18596738]
38. Stirewalt DL, Meshinchi S, Kopecky KJ, Fan W, Pogosova-Agadjanyan EL, Engel JH, Cronk MR, Dorcy KS, McQuary AR, Radich JP. Identification of genes with abnormal expression changes in acute myeloid leukemia. Genes Chromosomes Cancer. 2008; 47:8–20. [PubMed: 17910043]
39. Hollatz G, Grez M, Mastaglio S, Quaritsch R, Huenecke S, Ciceri F, Bonini C, Esser R, Klingebiel T, Koehl U. T cells for suicide gene therapy: activation, functionality and clinical relevance. J Immunol Methods. 2008; 331:69–81. [PubMed: 18155021]
40. Rao PE, Petrone AL, Ponath PD. Differentiation and expansion of T cells with regulatory function from human peripheral lymphocytes by stimulation in the presence of TGF-β. J Immunol. 2005; 174:1446–1455. [PubMed: 15661903]
41. Kalinski P, Hilkens CM, Wierenga EA, van der Pouw-Kraan TC, van Lier RA, Bos JD, Kapsenberg ML, Snijdewint FG. Functional maturation of human naive T helper cells in the absence of accessory cells. Generation of IL-4-producing T helper cells does not require exogenous IL-4. J Immunol. 1995; 154:3753–3760. [PubMed: 7706716]
42. Seder RA, Paul WE. Acquisition of lymphokine-producing phenotype by $CD4^+$ T cells. Annu Rev Immunol. 1994; 12:635–673. [PubMed: 7912089]
43. Jones L, Goldstein DR, Hughes G, Strand AD, Collin F, Dunnett SB, Kooperberg C, Aragaki A, Olson JM, Hodges AK. Assessment of the relationship between pre-chip and post-chip quality measures for Affymetrix GeneChip expression data. BMC Bioinformatics. 2006; 7:211. [PubMed: 16623940]
44. Brazma A, Hingamp P, Quackenbush J, Sherlock G, Spellman P, Stoeckert C, Aach J, Ansorge W, Ball CA, Vingron M. Minimum information about a microarray experiment (MIAME)—toward standards for microarray data. Nat Genet. 2001; 29:365–371. [PubMed: 11726920]

45. Irizarry RA, Hobbs B, Collin F, Beazer-Barclay YD, Antonellis KJ, Scherf U, Speed TP. Exploration, normalization, and summaries of high density oligonucleotide array probe level data. Biostatistics. 2003; 4:249–264. [PubMed: 12925520]
46. Storey JD, Tibshirani R. Statistical significance for genomewide studies. Proc Natl Acad Sci USA. 2003; 100:9440–9445. [PubMed: 12883005]
47. Xu XL, Olson JM, Zhao LP. A regression-based method to identify differentially expressed genes in microarray time course studies and its application in an inducible Huntington's disease transgenic model. Hum Mol Genet. 2002; 11:1977–1985. [PubMed: 12165559]
48. Zhao LP, Prentice R, Breeden L. Statistical modeling of large microarray data sets to identify stimulus-response profiles. Proc Natl Acad Sci USA. 2001; 98:5631–5636. [PubMed: 11344303]
49. Morey JS, Ryan JC, Van Dolah FM. Microarray validation: factors influencing correlation between oligo-nucleotide microarrays and real-time PCR. Biol Proc Online. 2006; 8:175–193.
50. Stirewalt DL, Mhyre AJ, Marcondes M, Pogosova-Agadjanyan E, Abbasi N, Radich JP, Deeg HJ. Tumour necrosis factor-induced gene expression in human marrow stroma: clues to the pathophysiology of MDS? Br J Haematol. 2008; 140:444–453. [PubMed: 18162123]
51. Ingenuity Pathway Analysis Online Help. IPA Learning Center, Frequently Asked Questions, FAQs about Statistical Calculations. [accessed August 10, 2009]. https//analyses.ingenuity.com/pa/info/help/.htm
52. Ingenuity Pathway Analysis Online Help. IPA Learning Center, Getting Started, Guidelines for publications. [accessed August 10, 2009]. https//analyses.ingenuity.com/pa/info/help/.htm
53. Livak KJ, Schmittgen TD. Analysis of relative gene expression data using real-time quantitative PCR and the 2(−Delta Delta C(T)) method. Methods. 2001; 25:402–408. [PubMed: 11846609]
54. Chen C, Mendez E, Houck J, Fan W, Lohavanichbutr P, Doody D, Yueh B, Futran ND, Upton M, Zhao LP. Gene expression profiling identifies genes predictive of oral squamous cell carcinoma. Cancer Epidemiol Biomarkers Prev. 2008; 17:2152–2162. [PubMed: 18669583]
55. Krolak JM, McClain D, Snyder SL, Fuchs P, Minton KW. 18 S ribosomal RNA is degraded during ribosome maturation in irradiated HeLa cells. Radiat Res. 1989; 118:330–340. [PubMed: 2727261]
56. Mori N, Mizuno D, Goto S. Increase in the ratio of 18S RNA to 28S RNA in the cytoplasm of mouse tissues during aging. Mech Ageing Dev. 1978; 8:285–297. [PubMed: 359949]
57. Payao SL, Smith MA, Winter LM, Bertolucci PH. Ribosomal RNA in Alzheimer's disease and aging. Mech Ageing Dev. 1998; 105:265–272. [PubMed: 9862234]
58. Tichy A, Zaskodova D, Rezacova M, Vavrova J, Vokurkova D, Pejchal J, Vilasova Z, Cerman J, Osterreicher J. Gamma-radiation-induced ATM-dependent signalling in human T-lymphocyte leukemic cells, MOLT-4. Acta Biochim Pol. 2007; 54:281–287. [PubMed: 17565390]
59. Kataoka Y, Murley JS, Baker KL, Grdina DJ. Relationship between phosphorylated histone H2AX formation and cell survival in human microvascular endothelial cells (HMEC) as a function of ionizing radiation exposure in the presence or absence of thiol-containing drugs. Radiat Res. 2007; 168:106–114. [PubMed: 17723002]
60. Amundson SA, Fornace AJ Jr. Monitoring human radiation exposure by gene expression profiling: possibilities and pitfalls. Health Phys. 2003; 85:36–42. [PubMed: 12852469]
61. Sudprasert W, Navasumrit P, Ruchirawat M. Effects of low-dose gamma radiation on DNA damage, chromosomal aberration and expression of repair genes in human blood cells. Int J Hyg Environ Health. 2006; 209:503–511. [PubMed: 16872898]
62. Satra M, Tsougos I, Papanikolaou V, Theodorou K, Kappas C, Tsezou A. Correlation between radiation-induced telomerase activity and human telomerase reverse transcriptase mRNA expression in HeLa cells. Int J Radiat Biol. 2006; 82:401–409. [PubMed: 16846975]
63. Amundson SA, Fornace AJ Jr. Gene expression profiles for monitoring radiation exposure. Radiat Prot Dosimetry. 2001; 97:11–16. [PubMed: 11763352]
64. Alsbeih G, Torres M, Al-Harbi N, Al-Buhairi M. Evidence that individual variations in TP53 and CDKN1A protein responsiveness are related to inherent radiation sensitivity. Radiat Res. 2007; 167:58–65. [PubMed: 17214516]

65. Daino K, Ichimura S, Nenoi M. Early induction of CDKN1A (p21) and GADD45 mRNA by a low dose of ionizing radiation is due to their dose-dependent post-transcriptional regulation. Radiat Res. 2002; 157:478–482. [PubMed: 11893252]
66. Turtoi A, Brown I, Oskamp D, Schneeweiss FH. Early gene expression in human lymphocytes after gamma-irradiation—a genetic pattern with potential for biodosimetry. Int J Radiat Biol. 2008; 84:375–387. [PubMed: 18464067]
67. Lu X, Yang C, Hill R, Yin C, Hollander MC, Fornace AJ Jr, Van Dyke T. Inactivation of gadd45a sensitizes epithelial cancer cells to ionizing radiation in vivo resulting in prolonged survival. Cancer Res. 2008; 68:3579–3583. [PubMed: 18483238]
68. Kis E, Szatmari T, Keszei M, Farkas R, Esik O, Lumniczky K, Falus A, Safrany G. Microarray analysis of radiation response genes in primary human fibroblasts. Int J Radiat Oncol Biol Phys. 2006; 66:1506–1514. [PubMed: 17069989]
69. Kondo K, Okuma K, Tanaka R, Matsuzaki G, Ansari AA, Tanaka Y. Rapid induction of OX40 ligand on primary T cells activated under DNA-damaging conditions. Hum Immunol. 2008; 69:533–542. [PubMed: 18718855]
70. Neef R, Gruneberg U, Barr FA. Assay and functional properties of Rabkinesin-6/Rab6-KIFL/MKlp2 in cytokinesis. Methods Enzymol. 2005; 403:618–628. [PubMed: 16473625]
71. Taniuchi K, Nakagawa H, Nakamura T, Eguchi H, Ohigashi H, Ishikawa O, Katagiri T, Nakamura Y. Down-regulation of RAB6KIFL/KIF20A, a kinesin involved with membrane trafficking of discs large homologue 5, can attenuate growth of pancreatic cancer cell. Cancer Res. 2005; 65:105–112. [PubMed: 15665285]
72. Yoshida K. Cell-cycle-dependent regulation of the human and mouse Tome-1 promoters. FEBS Lett. 2005; 579:1488–1492. [PubMed: 15733861]
73. Ayad NG, Rankin S, Murakami M, Jebanathirajah J, Gygi S, Kirschner MW. Tome-1, a trigger of mitotic entry, is degraded during G1 via the APC. Cell. 2003; 113:101–113. [PubMed: 12679038]
74. Lim HH, Surana U. Tome-1, wee1, and the onset of mitosis: coupled destruction for timely entry. Mol Cell. 2003; 11:845–846. [PubMed: 12718868]
75. Kraft C. Mitotic entry: tipping the balance. Curr Biol. 2003; 13:R445–446. [PubMed: 12781155]
76. Hsieh WJ, Hsieh SC, Chen CC, Wang FF. Human DDA3 is an oncoprotein down-regulated by p53 and DNA damage. Biochem Biophys Res Commun. 2008; 369:567–572. [PubMed: 18291097]
77. Jang CY, Wong J, Coppinger JA, Seki A, Yates JR 3rd, Fang G. DDA3 recruits microtubule depolymerase Kif2a to spindle poles and controls spindle dynamics and mitotic chromosome movement. J Cell Biol. 2008; 181:255–267. [PubMed: 18411309]
78. Sun WT, Hsieh PC, Chiang ML, Wang MC, Wang FF. p53 target DDA3 binds ASPP2 and inhibits its stimulation on p53-mediated BAX activation. Biochem Biophys Res Commun. 2008; 376:395–398. [PubMed: 18793611]
79. Hsieh PC, Chang JC, Sun WT, Hsieh SC, Wang MC, Wang FF. p53 downstream target DDA3 is a novel microtubule-associated protein that interacts with end-binding protein EB3 and activates beta-catenin pathway. Oncogene. 2007; 26:4928–4940. [PubMed: 17310996]
80. Abdollahi A, Domhan S, Jenne JW, Hallaj M, Dell'Aqua G, Mueckenthaler M, Richter A, Martin H, Debus J, Huber PE. Apoptosis signals in lymphoblasts induced by focused ultrasound. FASEB J. 2004; 18:1413–1414. [PubMed: 15231731]
81. Marples B, Wouters BG, Collis SJ, Chalmers AJ, Joiner MC. Low-dose hyper-radiosensitivity: a consequence of ineffective cell cycle arrest of radiation-damaged G_2-phase cells. Radiat Res. 2004; 161:247–255. [PubMed: 14982490]
82. Villa R, Zaffaroni N, Bearzatto A, Costa A, Sichirollo A, Silvestrini R. Effect of ionizing radiation on cell-cycle progression and cyclin B1 expression in human melanoma cells. Int J Cancer. 1996; 66:104–109. [PubMed: 8608951]

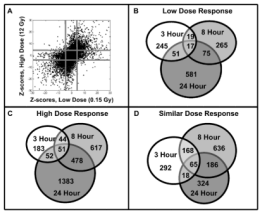

FIG. 1.

Expression changes after low- and high-dose radiation exposures. Panel A: Results from analyses at 8 h. The *x* axis shows Z scores for E_{low} vs. C_B analysis for all probe sets, while the *y* axis shows Z scores for the same probe sets from the E_{high} vs. C_B analysis. Thick lines represent Z-score boundary of +4.25 or −4.25. Panel B: Venn diagram showing the overlap of genes with significant expression changes at 3, 8 and 24 h after low-dose radiation exposure. Panel C: Venn diagram showing the overlap of genes with significant expression changes at 3, 8 and 24 h after high-dose radiation exposure. Panel D: Venn diagram showing the overlap of genes with similar expression changes at 3, 8 and 24 h after low- and high-dose radiation exposures.

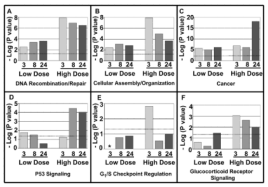

FIG. 2.

Functional and canonical pathways associated with radiation dose. Panel A: Relative significance obtained from IPA for DNA Recombination and Repair Functional category for low- and high-dose radiation exposures. Panels B and C: Relative significance for Cellular Assembly/Organization and Cancer Functional categories, respectively. Panel D: Relative significance obtained from IPA for p53 Signaling Canonical Pathway for low- and high-dose radiation exposures. Panel E and F: Relative significance for G_1/S Checkpoint Regulation and Glucocorticoid Receptor Signaling Canonical Pathways, respectively. Asterisk in panel E indicates a lack of genes contributing to G_1/S checkpoint regulation canonical pathway 3 h after low-dose irradiation. Dotted line represents the significance threshold.

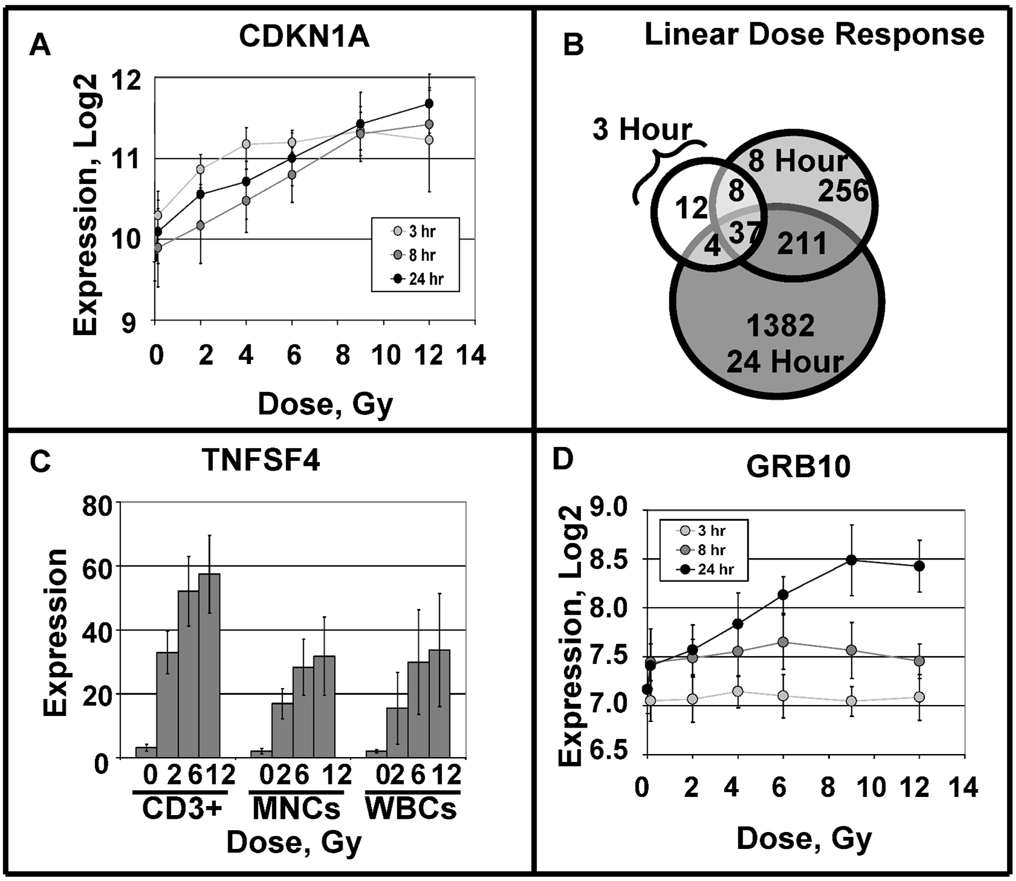

FIG. 3.

Linear dose-dependent gene expression changes. Panel A: Example of linear expression change in CDKN1A as a function of radiation dose. Error bars represent the standard deviation. Panel B: Venn diagram showing the overlap of genes with linear dose-dependent responses to radiation at 3, 8 and 24 h after exposure. Panel C: Expression of TNFSF4 in $CD3^+$ lymphocytes, mononuclear cells (MNCs), and white blood cell fraction (MNCs + granulocytes) 24 h after irradiation. Panel D: Example of time-dependent linear expression change in GRB10 as a function of radiation dose. Error bars represent the standard deviation (n = 8 donors for panels A, B, and D, n = 5 donors for panel C).

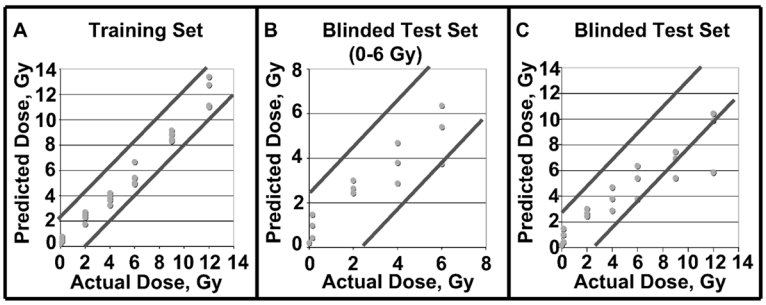

FIG. 4.

Development and validation of *in vitro* T-cell biodosimetry model based on expression of CDKN1A, PSRC1 and TNFSF4. Panel A: RNA-based assessment of predicted dose relative to actual dose used to develop the biodosimetry model (n = 5 donors, training set). Panel B: RNA-based assessment of predicted dose relative to the actual dose used to validate the biodosimetry model for sublethal doses of radiation (n = 3 donors, blinded testing set). Panel C: RNA-based assessment of predicted dose relative to the actual dose used to validate the biodosimetry model (n = 3 donors, blinded testing set).

TABLE 1

Summary of Dose-Specific Analyses

		3 h	8 h	24 h
Low dose	No. of genes	332	376	724
	Overlap	17: 12 induced, 5 repressed		
High dose	No. of genes	330	1189	1963
	Overlap	51: 27 induced, 24 repressed		
Similar	No. of genes	543	1105	593
	Overlap	65: 35 induced, 30 repressed		

TABLE 2

Radiation-Induced Expression Changes for the Top 10 Genes Identified by Linear Regression Analyses in T Cells

		Z-score linear analyses			Z-score multicovariate analyses				
Gene	**Affy ID**	**3 h**	**8 h**	**24 h**	**Gender**	**Age**	**Time**	**Dose*time**	**Dose**
KIF20A	218755_at	−7.69	−8.60	−9.42	1.28	0.52	2.94	1.40	−10.60
CDCA3	221436_s_at	−4.77	−8.98	−7.96	−1.02	0.95	1.29	−1.60	−9.25
PSRC1	201896_s_at	−6.55	−7.20	−7.82	−0.39	−0.43	3.12	2.23	−7.78
PRC1	218009_s_at	−6.20	−6.42	−7.43	1.31	2.23	4.19	−1.66	−7.51
SPAG5	203145_at	−4.74	−5.31	−7.42	−0.17	0.34	1.02	−2.72	−5.75
MDM2	211832_s_at	5.55	8.32	9.99	*6.90*	*4.46*	−1.34	0.41	6.22
PHLDA3	218634_at	5.09	10.85	10.72	1.43	*6.04*	−0.54	2.27	11.79
GADD45A	203725_at	5.19	11.78	11.27	*4.32*	*6.01*	−1.47	1.58	9.52
TNFSF4	207426_s_at	4.90	9.92	11.82	−1.50	1.51	−1.68	*5.34*	10.98
CDKN1A	202284_s_at	5.76	11.27	12.38	1.00	0.74	−0.80	1.99	12.58

Notes. Positive Z score indicates increased expression in the experimental cells relative to control (e.g., positive Z score for dose implies an increase expression in irradiated samples, while positive Z score for sex implies an increased expression in males relative to females). Italicized multicovariate Z scores highlight genes that show dose-dependent changes in expression that are also dependent upon other variables.

TABLE 3

Effects of Cellular Heterogeneity on Radiation-Induced Expression Changes Determined by qRT-PCR

	WBCs		MNCs		$CD3^+$	
Gene	***P***	R^2	***P***	R^2	***P***	R^2
CDKN1A	0.154	0.11	0.2005	0.09	0.6894	0.01
CDCA3	0.0001	0.57	0.0159	0.3	0.0438	0.42
GADD45A	0.0005	0.5	0.0006	0.51	0.0128	0.31
PSRC1	0.6892	0.01	0.5267	0.02	0.078	0.17
TNFSF4	0.0015	0.44	0.0003	0.55	<0.0001	0.67
KIF20A	NA[a]	NA	NA	NA	NA	NA

[a]No amplification.